ELSEVIER

Journal of Nuclear Materials 266–299 (1999) 312–317

journal of nuclear materials

Helium exhaust in ELMy H-mode plasmas with W-shaped pumped divertor of JT-60U

A. Sakasai *, H. Takenaga, N. Hosogane, S. Sakurai, N. Akino, H. Kubo, S. Higashijima, H. Tamai, N. Asakura, K. Itami, K. Shimizu

Japan Atomic Energy Research Institute, Naka Fusion Research Establishment, Department of Fusion Plasma Research, 801-1 Mukouyama, Naka-machi, Naka-gun, Ibaraki-ken, 311-0193, Japan

Abstract

By injecting a neutral beam of 60 keV helium (He) atoms as central fueling of helium into the ELMy H-mode plasmas, helium exhaust has been studied in the W-shaped pumped divertor on JT-60U. Efficient He exhaust was realized by He pumping using argon frosted cryopumps in the JT-60U new divertor. The He fueling rate by He beam injection was balanced with He pumping. In steady state, good He exhaust capability was successfully demonstrated in attached ELMy H-mode plasmas. A global particle confinement time of $\tau^*_{He} = 0.7$ s and $\tau^*_{He}/\tau_E = 4$ (τ_E: the energy confinement time) was achieved in attached plasmas, well within the range generally considered necessary for successful operation of a future fusion reactor, such as ITER. The enrichment factor of He was obtained to be about 1.0, which is five times larger than the ITER requirement of 0.2. Good He exhaust capability was also obtained in detached ELMy H-mode plasmas, which was comparable to one in attached plasmas. This result of the helium exhaust is sufficient to support a detached divertor operation on ITER.

Keywords: Helium exhaust; Helium ash; Helium beam; JT-60U; Divertor pumping; Helium gas puff

1. Introduction

Control of helium (He) ash is one of the key issues in future tokamak reactors, such as ITER and SSTR (Steady State Tokamak Reactor) [1]. ITER is designed to operate in H-modes with partially detached divertor or some other enhanced confinement regime for helium ash exhaust [2]. A detailed experimental database related to He level regulation and He ash removal should be developed to contribute to the determination of the device size and to the evaluation of the margin to ignition achievement. ELMy H-mode is attractive because of its capability of steady-state operation and particle exhaust by MHD relaxation at the plasma peripheral region.

Using a neutral beam of helium atoms as central fueling of helium or a short pulsed He gas puff as peripheral fueling, helium exhaust characteristics (He flux and neutral particle pressure in the divertor) have been studied to simulate He ash removal on TEXTOR [3] and JT-60 [4] in L-mode plasmas, and on JT-60U [5–7], DIII-D [8,9] and ASDEX-U [10] in ELMy H-mode plasmas. The previous study on JT-60U with He beam fueling indicated that He ash could be easily exhausted in ELMy H-mode and L-mode discharges with an open divertor configuration without pumping [6]. The deuterium flux is larger on the inner target than on the outer target on JT-60U [11]. The in–out asymmetry of He and deuterium flux in the divertor was studied in L-mode and ELMy H-mode plasmas [7]. The in–out asymmetry of He flux in the divertor during ELMy H-mode has been successfully controlled by changing neutral beam (NB) power and plasma current (I_P). Its characteristics are an important issue for He ash control.

Helium exhaust was so far performed by wall pumping due to gettering by solid target boronization (STB) in low density H-mode plasmas and low recycling di-

* Corresponding author. Tel.: +81 29 270 7342; fax: +81 29 270 7419; e-mail: sakasai@naka.jaeri.go.jp

0022-3115/99/$ – see front matter
PII: S0022-3115(98)00580-7

vertor [5]. In STB discharges, $\tau^*_{He}/\tau_E = 8$ (τ^*_{He}: the global particle confinement time of helium, τ_E: the energy confinement time) was successfully obtained [12]. The JT-60U divertor was modified from the open divertor to the W-shaped pumped divertor in February to May, 1997 [13]. The divertor modification enabled helium exhaust in high density H-mode plasmas and high recycling divertor with the divertor pumping. Helium exhaust experiments were performed to investigate the efficiency of helium exhaust with the W-shaped pumped divertor in attached and detached divertor discharges, and I_P and B_t reversed discharges.

2. W-shaped pumped divertor

Fig. 1 shows the poloidal cross section of an ELMy H-mode discharge in JT-60U after the installation of the new divertor (a) and the structure of the W-shaped pumped divertor (b). The new divertor consists of inclined divertor plates (vertical divertor) and a dome arranged in a W-shaped configuration, as well as inner baffles and outer baffles for the pumping duct [13]. The inclined target type divertor with a dome was adopted because of its effectiveness in achieving dense and cold divertor plasmas and baffling the back flow of neutral particles towards the boundary of main plasma. The dome is also expected to increase the pumping efficiency from the private flux region by compressing the deuterium molecule density and to function as a baffle for reducing the neutral particle flux to the X-point region at the same time. Carbon fiber composite (CFC) tiles are used for divertor plates, top tiles of the dome and baffling tiles at the divertor throat. For the other parts, graphite tiles are used.

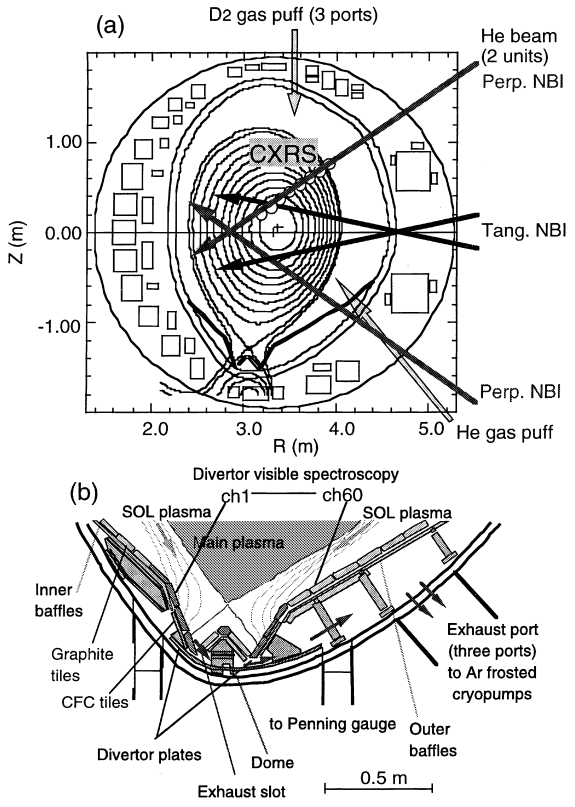

Fig. 1. (a) The cross section of an ELMy H-mode plasma in He exhaust experiments. The directions of He-NBI and heating NBI, the locations of He and D_2 gas puff, and the viewing position of CXRS for the He density measurements are shown. (b) The structure of W-shaped pumped divertor of JT-60U after divertor modification. Accumulated helium neutral particles near the inner strike point are removed through an exhaust slot with Ar frosted cryopumps via three exhaust ports.

An exhaust slot is located between the inner target plate and the dome. Three units of NBI cryopumps for divertor pumping are used to exhaust the gas through the slot. Fast movable shutter valves were installed in front of each cryopump to control timing and pumping speed of the divertor pump, which depends on opening rate of the valves.

The pumping speed was determined by measuring the neutral pressure without plasma. After deuterium gas was enclosed in the JT-60U vacuum vessel, pumping was started by opening the fast movable shutter valves of the divertor pump. The time evolution of neutral pressure at the main plasma and divertor (below the baffle plates, P_{baffle}) regions was measured with ionization gauges and Penning gauges. The effective pumping speed was estimated to be 13 m^3/s at $P_{baffle} = 0.06$ Pa for D_2. It was also estimated to be 13–15 m^3/s from the particle balance keeping the same density with and without pump by D_2 gas puff in ELMy H-mode discharges.

Helium exhaust is accomplished by condensing an argon (Ar) frost layer on the liquid helium cooled surface of three NBI cryopumps for divertor pumping between successive plasma discharges by injecting a known amount of Ar gas into the port chambers. In this manner, a layer of 1650 Pa m^3 per unit (surface area $\sim$15 m^2 per unit, 1.0 mm thick layer) before the first plasma and a layer of 240 Pa m^3 per unit (0.145 mm thick layer) between plasma discharges are condensed on the pumps, providing a measured pumping speed of 450 m^3/s for pure He and 700 m^3/s for a mixture gas of He:D_2 = 5:95 in steady state. Helium neutral particles accumulated in the private region are exhausted through the inner exhaust slot. Actually, the effective pumping speed is determined by the conductance of the exhaust slot and the under the dome. Therefore the effective pumping speed for He was experimentally evaluated to be 13 m^3/s. A total pumping capacity of the three Ar frosted NBI cryopumps was estimated to be 2325 Pa m^3 from the measurement.

In order to demonstrate steady-state helium exhaust, a long pulse He-NB injection is required. Thirty to forty

discharges with He-NB injection of about 5 s are possible without regeneration of the Ar frosted NBI cryopumps with a large pumping capacity in JT-60U. In DIII-D, the helium exhaust experiment was carried out with He-NB injection for 1.4 s and an in-vessel cryopump with an argon frost [9]. However, helium exhaust in a steady state was not achieved because of the limited He pumping capability.

3. Experimental setup

A tangential viewing charge-exchange recombination spectroscopy (CXRS) system provides radial density profiles of fully ionized helium as shown in Fig. 1(a). CXR emission of He II 468.52 nm ($n = 4$–3) is led to 0.5 m and 1.0 m Czerny–Turner spectrometers through 80 m pure quartz optical fibers. The detection system for He density profile measurement consists of image-intensified double linear photodiode arrays. The calibration of the CXRS system was performed by using an integrating sphere.

A set of spectrometers, a Langmuir probe array and an infrared television (IRTV) camera are used to measure the divertor characteristics. Recycling influx profiles of deuterium and He ions were derived, from the measured line intensities of D_α and He I (667.8 nm) with a 60 channel optical fiber array coupled to visible spectrometers as shown in Fig. 1(b). The neutral pressure of He and D_2 in the divertor region linked to the exhaust ports was measured by a Penning gauge below the outer baffles.

4. Helium exhaust in ELMy H-mode plasmas

The helium exhaust experiments were made possible with the JT-60U neutral beam system allowing 6.0 s steady-state He-NBI. Delivered powers on the order of 0.7–0.8 MW per unit (at 60 keV injection energy) are routinely available for up to 6.0 s pulses. Four units of NBI system, each consisting of 11 positive-ion source NBI units, are available for He-NBI.

In a situation with a simultaneous source and sink of helium, the global He particle balance equation is described by

$$dN_{He}/dt = S_{He} - Q_{He}, \quad (1)$$

where N_{He} is the total number of He ions in the plasma, S_{He} and Q_{He} are the instantaneous He source and exhaust rates, respectively. The He exhaust rate can be written as $N_{He}/\tau_{He} - R_{He}N_{He}/\tau_{He}$, where R_{He} is the global He recycling coefficient and $R_{He}N_{He}/\tau_{He}$ includes the recycling flux returning to the plasma and the exhausted flux. Then this equation takes on the familiar form

$$dN_{He}/dt = S_{He} - N_{He}/\tau^*_{He}, \quad (2)$$

where $\tau^*_{He} = \tau_{He}/(1 - R_{He})$. The general solution to this equation for a source turning on at time t_0 is

$$N_{He}(t) = N_{He}(t_0) + [S_{He}\tau^*_{He} - N_{He}(t_0)]\left\{1 - \exp\left[-\frac{(t - t_0)}{\tau^*_{He}}\right]\right\}, \quad (3)$$

provided S_{He} and τ^*_{He} are constant for $t > t_0$.

The enrichment factor of He was defined by $\eta_{He} = [P_{He}/2P_{D_2}]_{div}/[n_{He}/n_e]_{main}$, where $[P_{He}/2P_{D_2}]_{div}$ is the ratio of the He neutral pressure to the deuterium neutral pressure in the divertor and $[n_{He}/n_e]_{main}$ is the ratio of the He density to the electron density in the main plasma. It is a key parameter to reduce pumping speed of divertor pumping for future fusion reactors (i.e., $\eta_{He} \geqslant 0.2$), such as ITER. Both helium and fuel particles are simultaneously exhausted with divertor pumping. The higher He enrichment factor means that the required pumping speed is lower and leads us to reduce tritium inventory.

4.1. Attached plasmas

In the new divertor, effective He exhaust was demonstrated with He beam injection of $P_{He\text{-}NB} = 1.4$ MW, which corresponds to He fueling rate of 1.5×10^{20}/s (equivalent to 85 MW α heating) for 6 s into ELMy H-mode discharges. Fig. 2 shows the time evolution of the electron density, the fueled D_2 gas, total injected NB

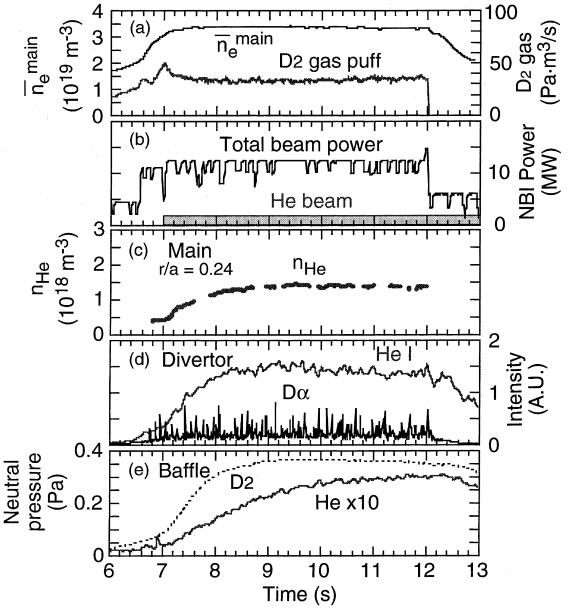

Fig. 2. Time evolution of the (a) plasma density and fueled D_2 gas, (b) total injected beam power and He beam power, (c) He density at $r/a = 0.24$, (d) He I and D_α intensities in the divertor, and (e) neutral pressure of He and D_2 below the outer baffles in an ELMy H-mode plasma. In steady state, the He source rate from the He beam injection is balanced by the exhaust rate.

power, He density, He I and D_α intensities in the divertor, the neutral pressure of He and D_2 below the outer baffles in an ELMy H-mode discharge ($I_P = 1.4$ MA, $B_t = 3.5$ T, $P_{NB} = 13$ MW, $q_{95\%} = 4.0$, $V_P = 58$ m^3). The line-averaged electron density in the main plasma is $\overline{n_e} = 3.4 \times 10^{19}$ m^{-3}, which corresponds to 0.5 of Greenwald density limit, and the central ion and electron temperatures are $T_i(0) = 3.2$ keV and $T_e(0) = 3.1$ keV in the ELMy H-mode plasma. Deuterium gas of about 30 Pa m^3/s is puffed to keep the electron density constant by a density feedback control. With He pumping, the He density measured by CXRS reached a steady state at 1.2 s after the start of the He beam injection, which was $n_{He} = 1.4 \times 10^{18}$ m^{-3} ($r/a = 0.24$) at $t = 12$ s. The He concentration reached 4% of the electron density in the main plasma and was kept constant for 4 s. This indicates that the He source rate (equivalent to 0.6 Pa m^3/s) from the He beam injection is balanced by the exhaust rate with He pumping. In this discharge, $\tau^*_{He} = 0.7$ s and $\tau^*_{He}/\tau_E = 4$ with $\tau_E = 0.18$ s and an H-factor ($\equiv \tau_E/\tau_E^{ITER\text{-}89P}$) = 1.3 were achieved, well within the range generally considered necessary for successful operation of future fusion reactors (i.e., $\tau^*_{He}/\tau_E \leqslant 10$), such as ITER.

The D_2 neutral pressure below the outer baffles reached a steady-state level of $P_{baffle\text{-}D_2} = 0.35$ Pa at $t = 9$ s. The He neutral pressure gradually increased and reached a steady-state level of $P_{baffle\text{-}He} = 0.03$ Pa at $t = 11$ s. The He enrichment factor was estimated to be 1.0 ± 0.2 from the He and D_2 neutral pressure at $t = 12$ s, which is five times larger than the ITER requirement of $\eta_{He} = 0.2$.

A similar ELMy H-mode discharge was performed closing the shutter valves in front of cryopumps. This condition of closed shutter valves is called 'without He pumping'. Without He pumping, the He concentration linearly increased up to 10% at 5 s after the start of the He beam injection, which was 2.5 times as much as that with pump in Fig. 3. Without He pumping, $\tau^*_{He} = 3.7$ s and $\tau^*_{He}/\tau_E = 21$ were obtained. However, a good enrichment factor of $\eta_{He} = 0.5$ was obtained without He pumping.

Helium exhaust experiments using a short He gas puff were performed to compare with those using He beam injection. Fig. 4 shows the time evolution of He density at $r/a = 0.66$ with and without He pumping using a short He gas puff. The line-averaged electron density of $\overline{n_e} = 2.7 \times 10^{19}$ m^{-3} is lower than the one in the above discharges. With and without He pumping, $\tau^*_{He} = 1.2$ s and $\tau^*_{He} = 10.2$ s were obtained, respectively. The time evolution of He density without pumping has two decay characteristics just after the He gas puff and later at $t = 9.0$ s by detailed viewing. This indicates that helium exhaust by 'the reservoir effect' is slightly observed even though without He pumping. The vacuum space of $V_{baffle} = 20$ m^3 below the outer baffles is filled with helium even when the pumping is not active, so that this space acts like a helium reservoir. Actually, helium exhaust is accomplished by the He pumping capability including the reservoir effect.

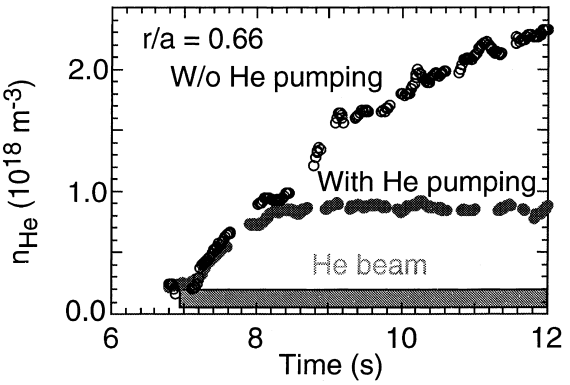

Fig. 3. Time evolution of the measured He density with and without He pumping. The He density with He pumping reaches a steady state at 1.2 s after the start of the He beam injection.

4.2. Detached plasmas

Effective He exhaust was also demonstrated with He beam injection into an ELMy H-mode discharge ($I_P = 1.7$ MA, $B_t = 3.5$ T, $P_{NB} = 12$ MW) with detachment. The line-averaged electron density in the main plasma is $\overline{n_e} = 6.7 \times 10^{19}$ m^{-3}, which corresponds to 0.8 of Greenwald density limit, the central ion and electron temperatures are $T_i(0) = 2.5$ keV and $T_e(0) = 2.3$ keV in the ELMy H-mode plasma. Deuterium gas of about 100 Pa m^3/s is puffed to keep the electron density constant. The He density reached a steady state ($n_{He} = 8.3 \times 10^{17}$

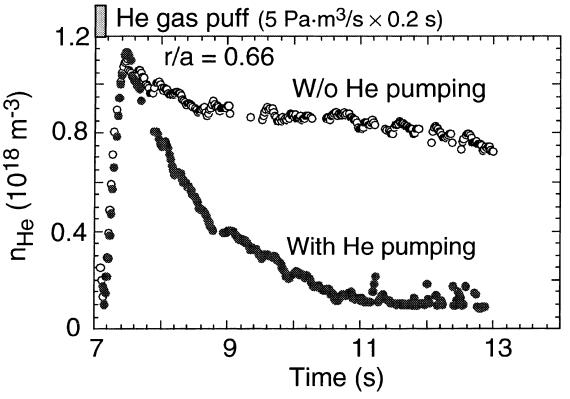

Fig. 4. Time evolution of measured He density with and without He pumping using a short He gas puff. The decay of the He density with He pumping is remarkably faster compared with the one without He pumping.

m^{-3} at $r/a = 0.66$) at 1.0 s after the start of the He beam injection with He pumping. The He concentration reached 1.3% of the electron density in the main plasma and was kept constant. In this discharge, $\tau^*_{He} = 0.5$ s and $\tau^*_{He}/\tau_E = 3$ (H-factor = 1.0) were achieved. In the other discharge ($I_P = 1.4$ MA, $B_t = 3.5$ T, $P_{NB} = 12$ MW, $\overline{n_e} = 5.8 \times 10^{19}$ m^{-3}, $\overline{n_e}/n^{Gr} = 0.8$), $\tau^*_{He} = 0.6$ s and $\tau^*_{He}/\tau_E = 4$ (H-factor = 1.0) were achieved. The He density with He pumping reached a steady state ($n_{He} = 9 \times 10^{17}$ m^{-3} at $r/a = 0.66$) and the He concentration reached 1.6% of the electron density in the main plasma. This result of the helium exhaust is sufficient to support a detached divertor operation on ITER.

In attached plasmas, an inboard-enhanced He flux and D flux profiles were observed. After a divertor detachment occurred, however, the inboard He and D fluxes decreased and the outboard fluxes increased, and then those flux profiles were almost in–out symmetry.

4.3. I_P and B_t reversal

The effect of the ion grad-B drift direction on He exhaust capability was investigated in the condition of reversed I_P and B_t because only inner exhaust slot was installed for divertor pumping in JT-60U. Fig. 5 shows He I brightness and D_α brightness profiles in the divertor in ELMy H-mode discharges. The inner He flux and D flux were higher than the outer flux at normal I_P and B_t (the ion grad-B drift direction towards the target) in an ELMy H-mode discharge ($I_P = 1.4$ MA, $B_t = 3.5$ T, $P_{NB} = 13$ MW, $\overline{n_e} = 3.4 \times 10^{19}$ m^{-3}, $\overline{n_e}/n^{Gr} = 0.5$) as shown in Fig. 5(a). On the other hand, an outboard-enhanced He flux and D flux were observed at reversed I_P and B_t (the ion grad-B drift away from the target) in an ELMy H-mode discharge ($I_P = 1.7$ MA, $B_t = 3.5$ T, $P_{NB} = 12$ MW, $\overline{n_e} = 3.5 \times 10^{19}$ m^{-3}, $\overline{n_e}/n^{Gr} = 0.4$) as shown in Fig. 5(b). The in–out asymmetry of the He and D flux profiles depends on the ion grad-B drift direction in these discharges.

Fig. 6 shows the comparison of the time evolution of the He density at normal and reversed I_P and B_t. The global particle confinement time of $\tau^*_{He} = 1.37$ s at reversed I_P and B_t is two times longer than that of $\tau^*_{He} = 0.7$ s at normal I_P and B_t. The same comparison in low density ELMy H-mode discharges of $I_P = 1.4$ MA, $B_t = 3.5$ T and $\overline{n_e} = 2.7 \times 10^{19}$ m^{-3} also indicates that τ^*_{He} at reversed I_P and B_t is 2.6 times longer. It was found that the He exhaust efficiency at reversed I_P and B_t was low because of the in–out asymmetry of the He flux and D flux profiles. The partial neutral pressure of D_2 and He below the outer baffles is very low. Particularly, the partial neutral pressure of $P_{baffle\text{-}D_2} = 0.047$ Pa is one order lower. The partial neutral pressure of $P_{baffle\text{-}He} = 0.014$ Pa is half the one at normal I_P and B_t. The neutral pressure drop in He and D_2 reflects the drop in He I and D_α brightness in Fig. 5. The neutral pressure below the outer baffles was low as expected because of the outboard enhanced particle flux profiles.

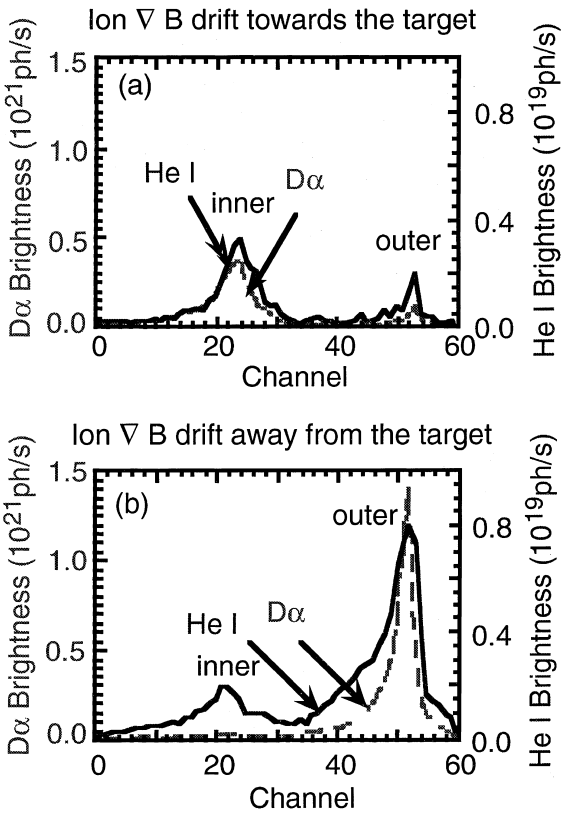

Fig. 5. Comparison of the brightness profiles of He I and D_α in the divertor region in the case of (a) ion grad-B drift direction towards the target and (b) ion grad-B drift direction away from the target.

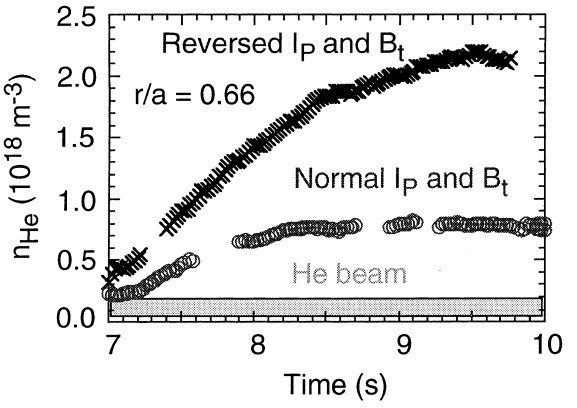

Fig. 6. Time evolution of the measured He densities at normal I_P and B_t (ion grad-B drift towards the target) and reversed I_p and B_t (ion grad-B drift away from the target) during He pumping.

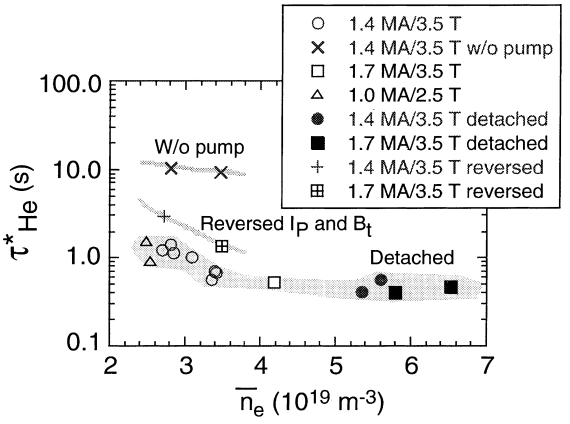

Fig. 7. The global particle confinement time of helium as a function of the line-averaged electron density in the main plasma in various operation modes (attached and detached divertor, reversed I_P and B_t, with and without He pumping).

4.4. Helium exhaust capability

The He exhaust capability was investigated in attached and detached plasmas. Fig. 7 shows the global particle confinement time τ^*_{He} as a function of the line-averaged electron density $\overline{n_e}$ in the main plasma. In attached plasmas, τ^*_{He} decreases and therefore the exhaust efficiency increases with increasing $\overline{n_e}$. The recycling flux of deuterium is not enhanced in low density ELMy H-mode discharges. Indeed, the enhancement of the recycling flux of He is difficult at $\overline{n_e}$ =2–3 × 10^{19} m^{-3}. The He recycling flux is exponentially enhanced with increasing $\overline{n_e}$. In detached plasmas, the in–out asymmetry with deuterium and He flux was relaxed. However, τ^*_{He} is comparable to the one in attached plasmas because of high recycling particle flux at the inner strike point in high density operation. At reversed I_P and B_t, τ^*_{He} is 2–3 times as long as compared to normal I_P and B_t.

5. Discussion and conclusion

Efficient He exhaust was realized with He pumping using Ar frosted NBI cryopumps the W-shaped pumped divertor on JT-60U. Neutral beams of 60 keV helium atoms were injected into ELMy H-mode plasmas for 6 s. In these discharges, the He source rate (equivalent to 0.6 Pa m^3/s) is balanced by the exhaust rate with He pumping. In steady state, good He exhaust capability ($\tau^*_{He}/\tau_E = 4$) was successfully demonstrated in ELMy H-mode plasmas. The enrichment factor of He was estimated to be about 1.0, which is five times larger than the ITER requirement of 0.2. The exhaust rate increased with the line averaged electron density. Even without He pumping, an enrichment factor of 0.5 was obtained by the geometry effect of the W-shaped divertor. It seems that the reflection of He neutral particles near the inner strike point is enhanced by the vertical divertor and the dome. These results strongly support the existing divertor designs of ITER.

In detached ELMy H-mode plasmas, τ^*_{He} is comparable to the one in attached plasmas because recycling particle flux is enhanced at the inner strike point in high density operation. Helium exhaust in detached plasmas could be an ITER divertor operation scenario. The inner leg pumping worked well for He exhaust because of the inboard-enhanced He flux and D flux at normal I_P and B_t (the ion grad-B drift direction towards the target). The in–out asymmetry with He and deuterium flux profiles strongly affects the He exhaust capability.

Acknowledgements

The authors would like to thank Drs M. Shimada, M. Nagami, R. Yoshino and M. Mori for useful discussion and advice. They would like to acknowledge the continuous support of Drs H. Kishimoto, A. Funahashi and M. Azumi and the contributions of JT-60 team.

References

[1] M. Kikuchi, Nuclear Fusion 30 (1990) 265.
[2] ITER Detail Design Report, Nov. 1996.
[3] D.L. Hillis et al., Phys. Rev. Lett. 65 (1990) 2382.
[4] H. Nakamura et al., Phys. Rev. Lett. 67 (1991) 2658.
[5] A. Sakasai et al., in: Proceedings of the 15th International Conference on Plasma Physics and Controlled Nuclear Fusion Research, vol. 2, Seville, 1994, IAEA, Vienna, 1995, p. 95.
[6] A. Sakasai et al., J. Nucl. Mater. 220–222 (1995) 405.
[7] A. Sakasai et al., in: Proceedings of the 16th International Conference on Fusion Energy, vol. 1, Montreal, 1996, IAEA, Vienna, 1997, p. 789.
[8] M.R. Wade et al., J. Nucl. Mater. 220–222 (1995) 178.
[9] M.R. Wade et al., in: Proceedings of the 16th International Conference on Fusion Energy, vol. 1, Montreal, 1996, IAEA, Vienna, 1997, p. 801.
[10] H.-S. Bosh et al., in: Proceedings of the 16th International Conference on Fusion Energy, vol. 1, Montreal, 1996, IAEA, Vienna, 1997, p. 809.
[11] N. Asakura et al., Nucl. Fusion 37 (1996) 795.
[12] D. Reiter et al., Nucl. Fusion 30 (1990) 2141.
[13] N. Hosogane et al., in: Proceedings of the 16th International Conference on Fusion Energy, vol. 3, Montreal, 1996, IAEA, Vienna, 1997, p. 555.